remote sensing

MDPI

Article

The August 2019 Piton de la Fournaise (La Réunion Island) Eruption: Analysis of the Multi-Source Deformation Pattern Detected through Sentinel-1 DInSAR Measurements

Emanuela Valerio [1,*], Claudio De Luca [1], Riccardo Lanari [1], Mariarosaria Manzo [1] and Maurizio Battaglia [2]

[1] Istituto per il Rilevamento Elettromagnetico dell'Ambiente, IREA-CNR, 80124 Napoli, Italy; deluca.c@irea.cnr.it (C.D.L.); lanari.r@irea.cnr.it (R.L.); manzo.mr@irea.cnr.it (M.M.)
[2] Dipartimento di Scienze della Terra, Sapienza Universita di Roma, 00185 Rome, Italy; maurizio.battaglia@uniroma1.it
* Correspondence: valerio.e@irea.cnr.it

Contents of this File

Figures S1 to S6

Introduction

This supplement contains supporting material aimed at providing additional information on the presented contents. In Figure S1 we report the results obtained by gradually increasing the number of the volcanic sources, and by considering two sources (i.e., one sill-like source and one dike), three sources (i.e., one sill-like source and two dikes) and four sources (i.e., one sill-like source and three dikes). Moreover, we also report in Figures S2 to S6 detailed information (i.e., parameter uncertainties and tradeoffs of the retrieved sources) on the final performed analytical modelling (see Figure 4) of the volcanic sources responsible for the observed ground displacements.

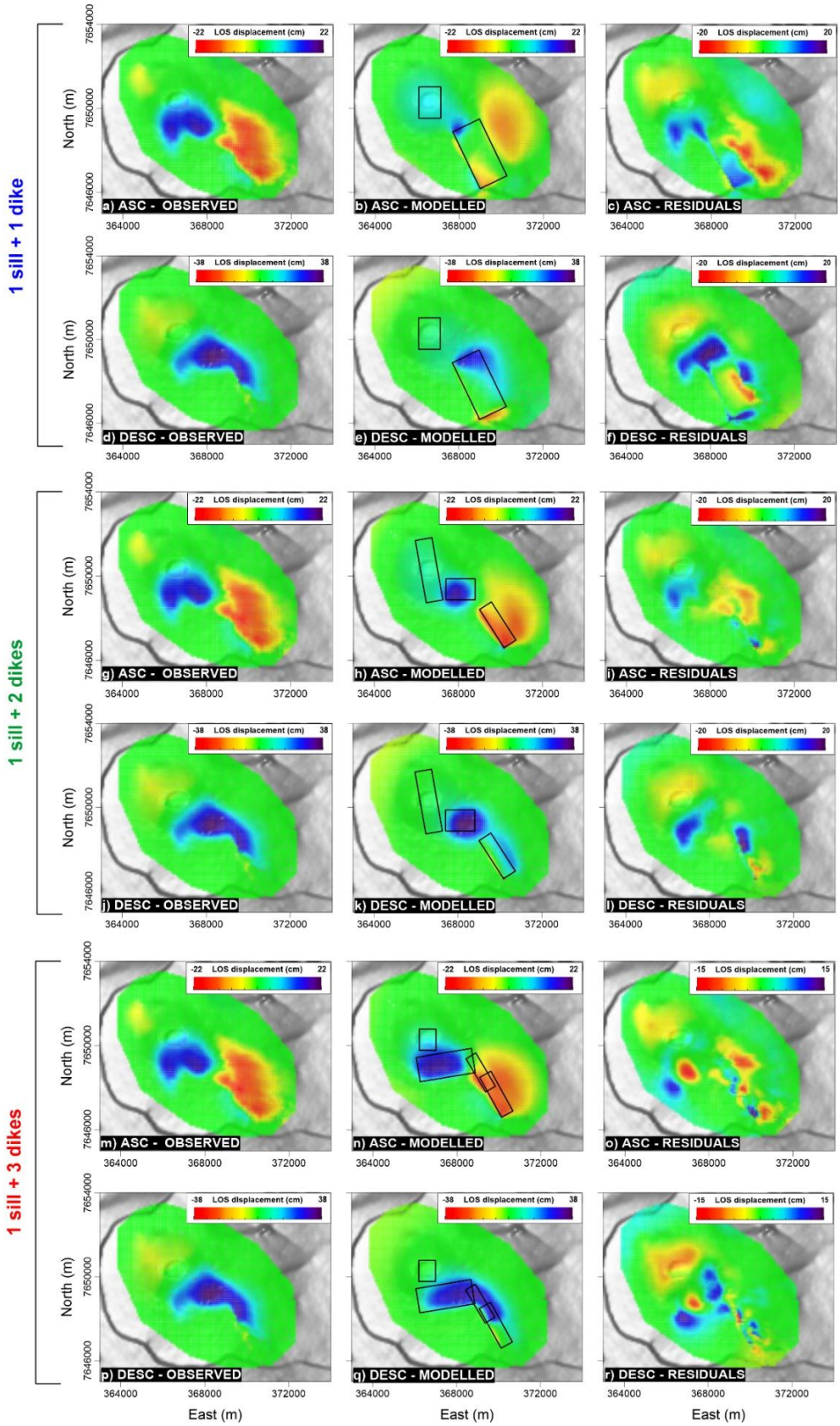

Figure S1. Inversion results relevant to three scenarios obtained by gradually increasing the number of the volcanic sources, by considering two, three and four sources. In particular, in the first scenario we consider one sill-like source and one dike; we report the line-of-sight (LOS) projected displacement maps for S1 ascending (**a**) and descending (**d**) orbits interferograms and, in (**b**) and (**e**), the corresponding LOS projected displacement maps computed from the retrieved analytical models.

The related residual maps are shown in (**c**) and (**f**), respectively. In the second scenario we consider one sill-like source and two dikes; we report the line-of-sight (LOS) projected displacement maps for S1 ascending (**g**) and descending (**j**) orbits interferograms and, in (**h**) and (**k**), the corresponding LOS projected displacement maps computed from the retrieved analytical models. The related residual maps are shown in (**i**) and (**l**), respectively. In the third scenario we consider one sill-like source and three dikes; we report the line-of-sight (LOS) projected displacement maps for S1 ascending (**m**) and descending (**p**) orbits interferograms and, in (**n**) and (**q**), the corresponding LOS projected displacement maps computed from the retrieved analytical models. The related residual maps are shown in (**o**) and (**r**), respectively. All the retrieved solutions are also marked by black rectangles. Note also that the reported maps are superimposed on the 1 arcsec Shuttle Radar Topography Mission (SRTM) Digital Elevation Model (DEM) of the zone.

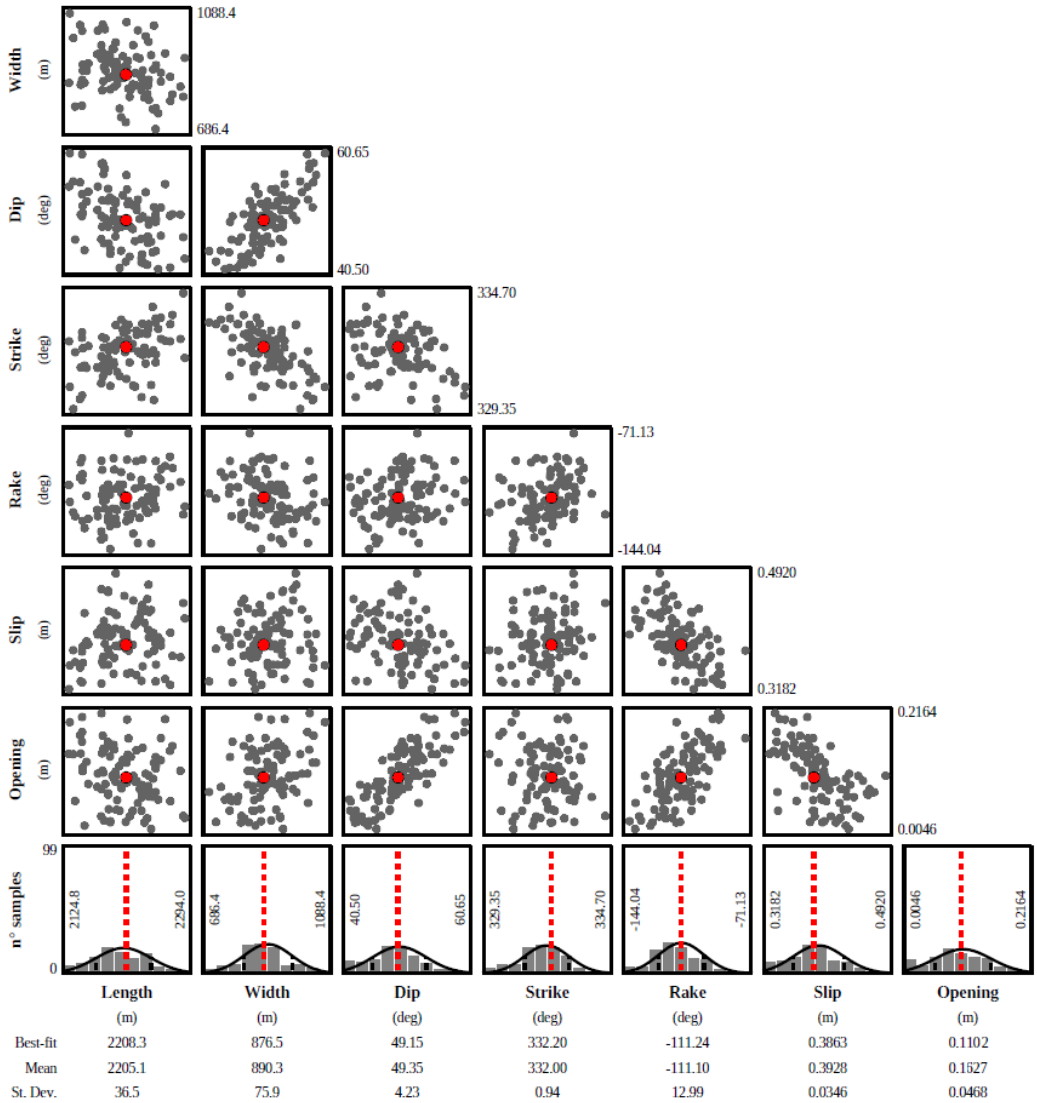

Figure S2. D1 dike: parameter uncertainties and tradeoffs. Parameter uncertainties and tradeoffs for the modelled D1 source retrieved by Sentinel-1 measurements (see Figure 4). Histograms and scatterplots show the a-posteriori probability distribution of fault parameters, and the trade-offs between parameters, respectively.

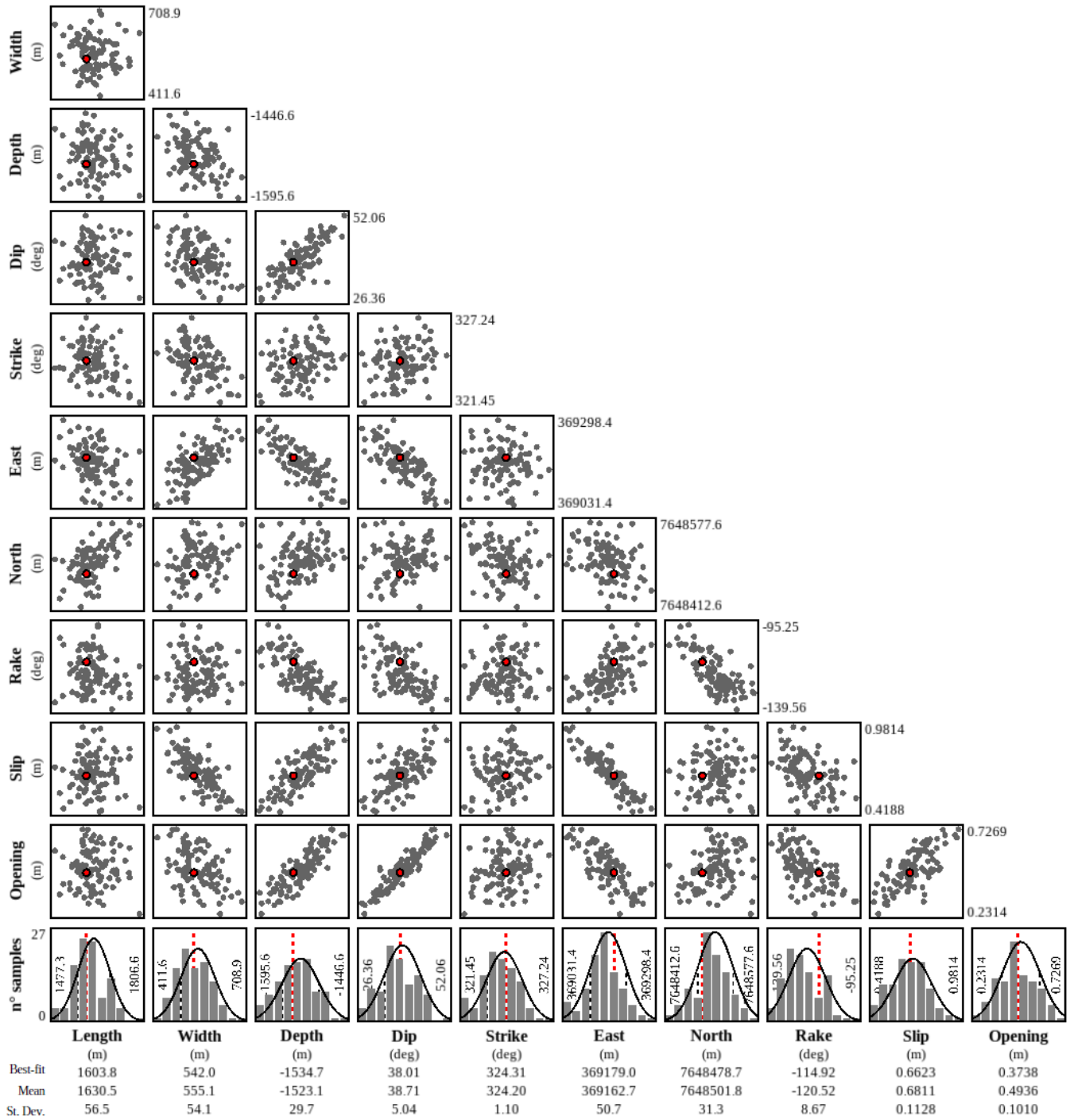

Figure S3. D2 dike: parameter uncertainties and tradeoffs. Parameter uncertainties and tradeoffs for the modelled D2 source retrieved by Sentinel-1 measurements (see Figure 4). Histograms and scatterplots show the a-posteriori probability distribution of fault parameters, and the trade-offs between parameters, respectively.

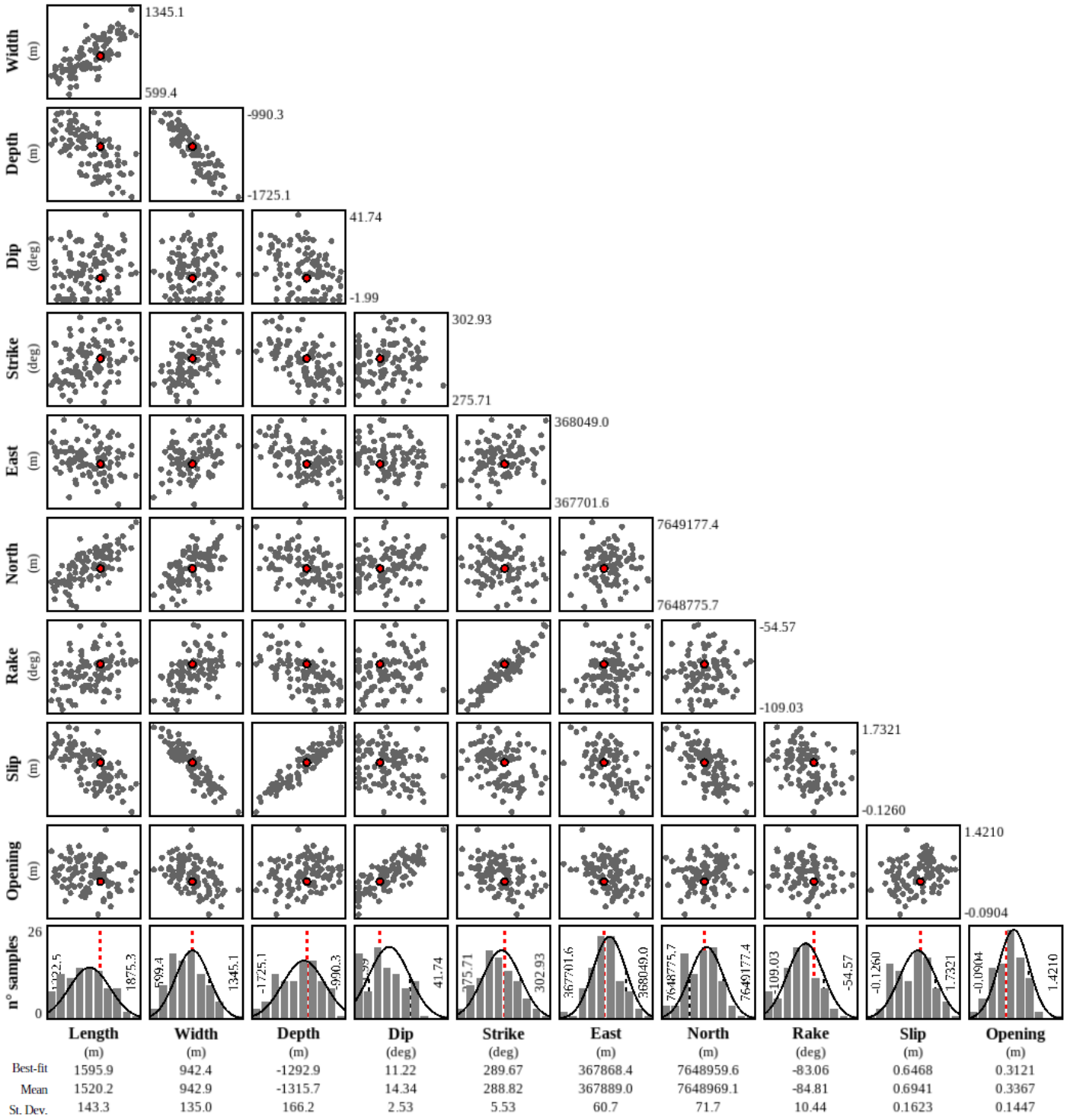

Figure S4. D3 dike: parameter uncertainties and tradeoffs. Parameter uncertainties and tradeoffs for the modelled D3 source retrieved by Sentinel-1 measurements (see Figure 4). Histograms and scatterplots show the a-posteriori probability distribution of fault parameters, and the trade-offs between parameters, respectively.

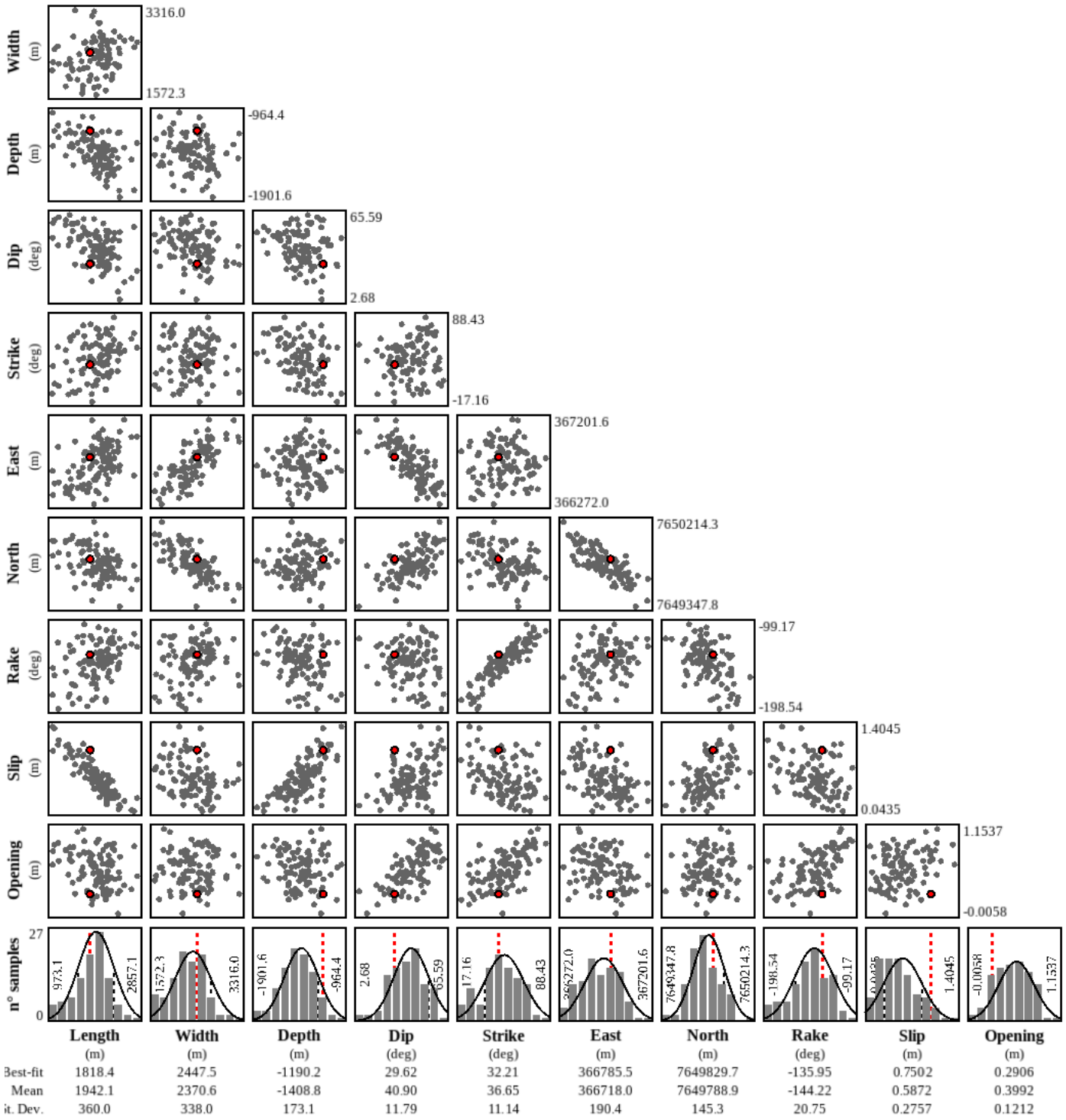

Figure S5. D4 dike: parameter uncertainties and tradeoffs. Parameter uncertainties and tradeoffs for the modelled D4 source retrieved by Sentinel-1 measurements (see Figure 4). Histograms and scatterplots show the a-posteriori probability distribution of fault parameters, and the trade-offs between parameters, respectively.

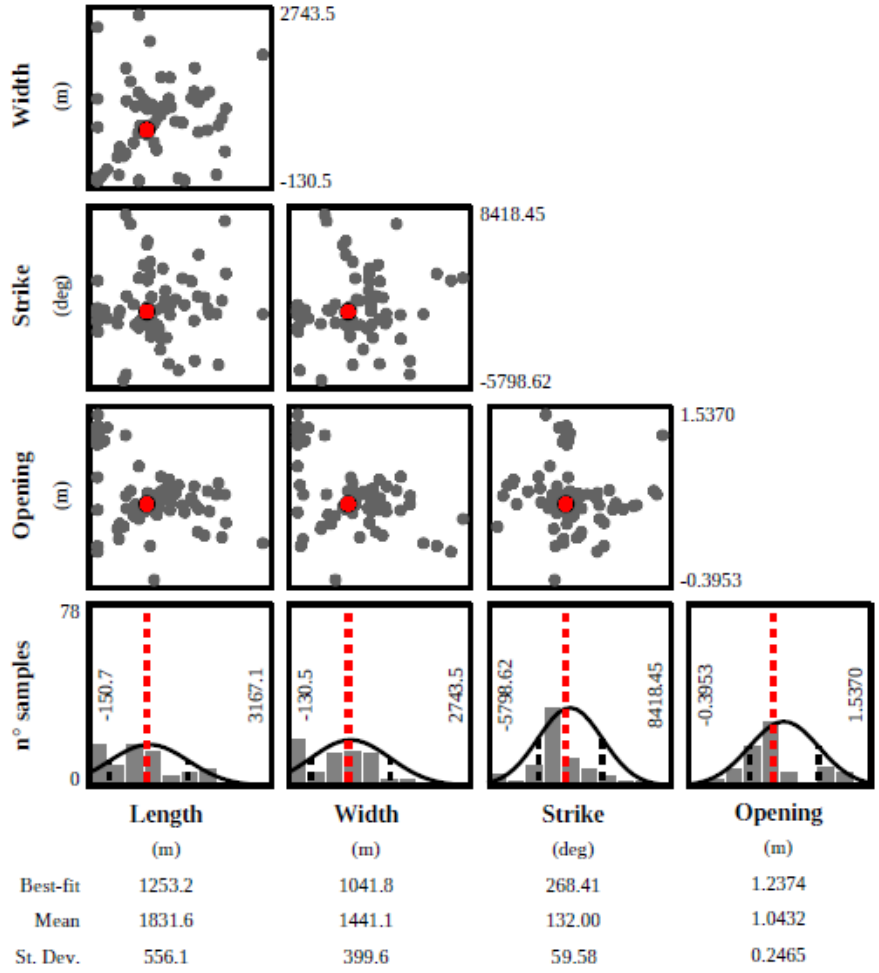

Figure S6. Sill-like source: parameter uncertainties and tradeoffs. Parameter uncertainties and tradeoffs for the modelled sill-like source retrieved by Sentinel-1 measurements (see Figure 4). Histograms and scatterplots show the a-posteriori probability distribution of fault parameters, and the trade-offs between parameters, respectively.

DATA SET

The generated LOS displacement maps referred to the pre- and co-eruptive phases are also attached in the kmz format:

InU_ASC_20190802_20190814.kmz
InU_DESC_20190802_20190814.kmz
InW_ASC_20190802_20190814.kmz
InW_DESC_20190802_20190814.kmz
VerticalComponent.kmz
EastWestComponent.kmz

The exploited seismicity is referred to the 2–15 August 2019 time interval and is attached in the txt format:

Seismicity.txt

All the datasets generated and/or analyzed during the present study are available in the Zenodo repository (doi: 10.5281/zenodo.6255531).